Brief communication: Use of lightweight and low-cost steel net electrodes for electrical resistivity tomography (ERT) surveys performed on coarse-blocky surface environments

Mirko Pavoni [1], L. Peruzzo [1], J. Boaga [1], A. Carrera [1], I. Barone [1] and A. Bast [2,3]

[1] Department of Geosciences, Università degli Studi di Padova, Padova, Italy.
[2] WSL Institute for Snow and Avalanche Research SLF, Permafrost Research Group, Davos Dorf, Switzerland.
[3] Climate Change, Extremes and Natural Hazards in Alpine Regions Research Center CERC, Davos Dorf, Switzerland.

Correspondence to: Mirko Pavoni (mirko.pavoni@unipd.it)

Abstract. ERT is a widely used geophysical technique for characterizing various mountainous environments where land surfaces consist of coarse blocks and debris (e.g., rock glaciers). In these conditions, installing steel spike electrodes is both challenging and time-consuming, and achieving acceptable grounding resistance between the electrodes and the surface is difficult. In this work, we successfully tested the performance and the durability of an alternative electrode that is more robust, lightweight, and cost-effective than the recently proposed textile electrode. A stainless-steel net and sponge are used to create small bags that can be easily inserted between the blocks and later removed.

1 Introduction

Electrical Resistivity Tomography (ERT) is one of the most widely used geophysical methods for the characterization of various study environments (e.g., Boaga et al., 2018; Deiana et al., 2022; Carrera et al., 2024; Pavoni et al., 2024; Peruzzo et al., 2024; Uhlemann et al., 2024), as data acquisition is generally rapid and relatively straightforward (Binley, 2015). Thanks to the development of open- reliable source inversion techniques, the distribution of electrical properties in the subsurface can be efficiently reconstructed (Rücker et al., 2017). The reliability of resistivity models is closely linked to the quality of acquired data, which in turn depends on achieving good electrical contact between electrodes and soil (Pavoni et al., 2022). This resistance is part of the overall grounding resistance, which depends on soil resistivity, electrode geometry, and the quality of contact with the ground. Grounding resistance plays a crucial role in ensuring effective current injection and reliable ERT measurements (Binley and Slater, 2020). For this reason, modern electrical resistivity meters perform an automated check before acquisition by injecting a low current through each electrode, measuring the resulting voltage drop to estimate electrode resistance, and identifying poorly coupled electrodes. Therefore, electrodes must be made from highly conductive materials. Common choices include graphite, copper, and stainless steel (Rücker and Günther, 2011). Graphite offers low resistance but poor mechanical performance. Copper has excellent conductivity but tends to oxidize, reducing effectiveness over time. Stainless steel, though less conductive, does not oxidize, has good mechanical strength, and is cost-effective (Reynolds, 2011). For these reasons, stainless-steel spike electrodes, typically 30–40 cm in length and 1–2 cm in diameter, are widely used in ERT surveys (Rücker and Günther, 2011). While easy to install in fine soils, their deployment in coarse-blocky terrains such as landslide deposits or rock glaciers is often difficult and time-consuming (Bast et al., 2024). Removal can also be problematic when electrodes become embedded between blocks. Even when physical contact is good, sponges soaked in salt water are often used to reduce contact resistance (Pavoni et al., 2022).

To facilitate the installation of ERT arrays in rock glaciers, Buckel et al. (2023) proposed an alternative electrode (https://depatisnet.dpma.de/DepatisNet/depatisnet?action=bibdat&docid=DE102021110721A1) consisting of a conductive textile sachet filled with sand. These fist-sized electrodes can be easily inserted between blocks, wetted with salt water, and removed after use. Their performance was tested by Bast et al. (2024), confirming their reliability. However, the conductive textile used in both studies contains copper and nickel, which are prone to oxidation, potentially reducing performance over time (Bast et al., 2024). Moreover, each electrode costs approximately €15 and weighs around 250–300 g, making it relatively expensive and heavy.

In this work, we propose a lightweight stainless-steel net electrode filled with a carwash sponge. This design uses oxidation-resistant material, significantly reduces weight and cost, and improves the mechanical robustness of the electrode compared to textile-based solutions. We tested the performance of the newly developed stainless-steel net electrode by conducting ERT surveys at the same coarse-blocky sites used by Bast et al. (2024), and compared the results with those obtained using traditional stainless-steel spikes coupled with sponges. In addition, we tested their long-term performance by employing them on a permanent ERT monitoring line installed on a rock glacier.

2 Site description

The proposed stainless-steel net electrodes were tested in typical high mountain environments characterized by coarse blocky and debris-covered surfaces, including a landslide deposit (Marocche di Drò), an inactive rock glacier (Sadole rock glacier), and an active rock glacier (Flüela rock glacier). For detailed site descriptions, maps, and images, we refer to Bast et al. (2024).

The landslide deposit known as the Marocche di Drò (Trentino, Italy; 45.983° N, 10.941° E) consists of a chaotic surface accumulation of calcareous blocks and debris (limestone), underlain by a more heterogeneous sedimentary body (Weidinger et al., 2014). The test survey was carried out along the same profile previously investigated by Bast et al. (2024).

The Sadole rock glacier (Trentino, Italy; 46.242° N, 11.592° E) features a surface dominated by large blocks and coarse debris of ignimbritic volcanic origin (Pavoni et al., 2023). According to Bast et al. (2024), the central lobe hosts a frozen layer at approximately 10 m depth. Our comparison test was conducted along the first half of their original survey line.

The Flüela rock glacier (Grisons, Switzerland; 46.746° N, 9.951° E) is characterized by a chaotic mixture of metamorphic blocks and boulders (amphibolites and paragneisses), with some interspersed patches of finer sediments (Boaga et al., 2024). The comparative measurements were performed along the upper section of the profile investigated by Bast et al. (2024).

3 Methods

3.1 Stainless steel-net electrodes

To replicate the size of the textile electrode (Buckel et al., 2023), each stainless-steel net electrode was constructed by cutting 35 × 35 cm square sheets from a thin commercial stainless-steel mesh (Fig. 1a). The net was shaped into a fist-sized pouch filled with a car-wash sponge and sealed using a standard electrician's cable tie. Each electrode weighs approximately 50 g, i.e., one-fifth the weight of traditional stainless-steel spike or textile electrodes, and the material cost is around € 3–4, i.e., one-quarter of the cost of textile electrode design.

3.2 Data acquisition

ERT data were collected using a Syscal Pro resistivity meter (Iris Instruments, Orléans, France; www.iris-instruments.com) with 24-electrode arrays and site-specific electrode spacings: 5 m at Marocche di Drò, 3.5 m at Sadole, and 2 m at Flüela. A dipole–dipole acquisition scheme was adopted with variable electrode skips, as described in Pavoni et al. (2023), and included reciprocal measurements, i.e., with current and potential dipoles interchanged (Binley and Slater, 2020).

For each survey line, measurements were performed using traditional stainless-steel spike electrodes (combined with sponges; Fig. 1b), and then repeated using the proposed stainless-steel net electrodes (Fig. 1c). In both cases, saltwater was applied to improve the galvanic contact between the electrodes and the coarse blocky surface (Pavoni et al., 2022). The two electrode types were installed in the same locations between blocks and boulders (Fig. 1b–c), with approximately 0.5 L of saltwater poured on each electrode prior to acquisition.

At the Sadole rock glacier site, net electrodes were installed for a permanent ERT monitoring line to assess their long-term performance. We compared measurements (grounding resistance, injected current, and reciprocal error) acquired in June 2024 and June 2025.

3.3 Data processing

At each test site, grounding resistance was measured prior to data acquisition for both electrode types. To compare these values, grounding resistance measurements from each electrode pair were visualized using histograms. Dataset quality was assessed by calculating the reciprocal error for each quadrupole (Tso et al., 2017), and histograms were also used to compare the distribution of injected currents and reciprocal errors across the different electrode types.

The apparent resistivity pseudosections were compared by calculating the differences in measured resistance values between the two datasets. Additionally, apparent resistivity values were analysed using scatterplots with linear regression lines and corresponding R^2 values. Each dataset was filtered using a reciprocal error threshold to ensure a homogeneous distribution of data points across the profile (Pavoni et al., 2023). This value was used as expected data error in the inversion process, which was carried out using the open-source software ResIPy (Blanchy et al., 2020). Note that, only the quadrupoles common to both datasets after filtering were used for the inversion process (Bast et al., 2024). The resulting inverted resistivity models were then compared by analysing both the section images and the cell-wise resistivity values from the inversion mesh using scatterplots with regression lines and R^2 values.

4 Results and interpretation

In the comparative test at the Marocche di Drò site, the grounding resistances measured with the two types of electrodes were very similar (Fig. 2a), with values < 200 kΩ (most being < 100 kΩ), ensuring acceptable conditions to acquire ERT measurements in this challenging environment (Pavoni et al., 2022). These favorable resistance values also resulted in optimal injected currents, which were consistently above 3 mA, as shown in Fig. 2b. This is further confirmed by the quality of the acquired data: most of the measured quadrupoles (85% for spike and 90% for net electrodes) show a reciprocal error < 5% (Fig. 2c), which was chosen as a threshold to filter the datasets and used as the expected error in the inversion processes. As highlighted in the scatterplots (Fig. 3a and 3g), there is a very high correlation between the measured apparent resistivities and the inverted resistivities, both showing $R^2 = 0.99$. The obtained apparent (Fig. 3d) and inverted resistivity sections (Figs. 3j and 3m) are nearly identical and allow for the reconstruction of the known structure of the landslide deposit (Weidinger et al., 2014), where large blocks with extensive air voids are characterized by high resistivity values near the surface. At greater depths, resistivity values decrease significantly, confirming the presence of more heterogeneous and finer sediments.

At the Sadole rock glacier, the measured grounding resistances were significantly improved using the net-electrodes (Fig. 2d). With the spike-electrodes array, almost half of the grounding resistances have values > 100 kΩ, and > 50 % of the values are higher > 200 kΩ. In contrast, in the case of net electrodes, the grounding resistance values are clearly lower, which enables the injection of higher currents (fig. 2e) and consequently the acquisition of a higher-quality dataset (Fig. 2e). In the dataset acquired with the net electrodes, more than half of the quadrupoles exhibit a reciprocal error below 1%, and only four quadrupoles exceed 5%. Nonetheless, the spike electrodes also yielded a high-quality dataset, with 90% of the quadrupoles showing a reciprocal error below 5%. Despite these minor differences in data quality, the same filtering threshold (reciprocal error > 5%) was applied to both datasets and used as the expected data error during the inversion process. As illustrated in Figures 3b and 3e, the measured apparent resistivities and the corresponding inverted values exhibit a strong correlation, albeit slightly lower than at the Marocche di Drò site ($R^2 = 0.91$ for apparent resistivities and $R^2 = 0.93$ for inverted values). Once again, the apparent (Fig. 3e) and inverted resistivity sections (Figs. 3k and 3n) are nearly identical and clearly reveal the presence of a high-resistivity frozen layer at approximately 10 m depth (Bast et al., 2024).

The measured grounding resistances at the Flüela rock glacier site (Fig. 2g) were generally higher than at the other two sites. With both electrode types, more than half of the electrodes exhibited grounding resistances > 200 kΩ. As a consequence, the injected currents (Fig. 2h) were consistently lower compared to those recorded at the Marocche di Drò and Sadole sites. This is reflected in the dataset quality (Fig. 2i), where only 78% of the acquired quadrupoles in both datasets exhibit a reciprocal error < 5%, and 90% remain below 10%, which was adopted as the expected error for the inversion process. The correlation between apparent resistivities obtained using the two electrode types is also lower than at the other sites (Fig. 3c, $R^2 = 0.80$). Accordingly, the inverted resistivities from the resulting models show a reduced correlation as well ($R^2 = 0.88$; Fig. 3i). Despite minor differences, both the apparent (Fig. 3f) and inverted resistivity sections (Figs. 3l and 3o) derived from the two electrode types consistently delineate the same subsurface structure: a high-resistivity permafrost body a few meters below the surface in the first half of the profile (x < 20 m). Variations appear at greater depths, where resistivities in Fig. 3l are higher than in Fig. 3o, and toward the front of the array (x > 25 m), where lower values indicate unfrozen ground.

Finally, Figures 2j–2l clearly show that, despite the net electrodes being left in situ (Sadole rock glacier) for over a year, their performance remained essentially unchanged. They allowed for the acquisition of comparable grounding resistance values and injected currents, as well as similar reciprocal errors in the datasets collected in June 2024 and June 2025.

4 Discussion and conclusions

The results confirm that lower grounding resistance enhances current injection and enables the acquisition of higher-quality ERT data (Pavoni et al., 2022). Among the test sites, Marocche di Drò showed the best performance, with the lowest grounding resistance, highest injected currents, and best data quality. At Sadole rock glacier, grounding resistances—especially with net electrodes—were also low, supporting consistently good data quality. In contrast, at the Flüela rock glacier, we exhibited moderately higher grounding resistances with both electrode types, resulting in lower injected currents and reduced data quality. Nevertheless, the datasets from Flüela remained suitable for processing after applying a 10% reciprocal error threshold, which is acceptable given the site's challenging surface conditions. Performance differences likely reflect subsurface lithologies: limestone at Marocche di Drò favors galvanic contact more than ignimbrite (Sadole) or amphibolite/paragneiss (Flüela) (Duba et al., 1978). Additionally, sites with lower grounding resistance and better data quality exhibited stronger correlations between apparent and inverted resistivities measured with the two electrode types. At Marocche di Drò, both datasets yielded nearly identical results. At Sadole, the correlation remained high despite slightly lower data quality, and the inverted models were still closely aligned. At Flüela, both correlations declined modestly ($R^2 = 0.88$), yet the inverted resistivity models consistently resolved the same near-surface permafrost structure. Considering all this, the proposed stainless steel-net electrodes produce results equivalent to those obtained with conventional steel-spike electrodes, and represents a lightweight and low-cost reliable solution to collect ERT datasets in coarse-blocky surface environments. The steel-net electrodes retain all the advantages of the textile electrodes proposed by Buckel et al. (2023), namely facilitating and accelerating the deployment of ERT investigation lines without compromising the quality of the final results. At the same time, they overcome the limitations of the conductive textile presented by Bast et al. (2024): the stainless-steel net is more durable (resistant to oxidation), significantly less expensive and lighter (easier to transport in challenging mountain terrains), and mechanically more robust than the conductive textile, which is prone to tearing when inserted between blocks.

Furthermore, having verified that the performance of the net electrodes at the Sadole rock glacier monitoring site remains stable over time (one year), they can be considered a viable alternative to traditional steel spikes for permanent ERT transect installations, which represent a powerful tool to monitor seasonal and long-term permafrost variations. In contrast, textile electrodes (Buckel et al., 2023) are unsuitable for this target due to oxidation issues that compromise their durability.

Future development of this work is to test the stainless-steel net electrodes for induction polarization measurements, both in the time and frequency domains.

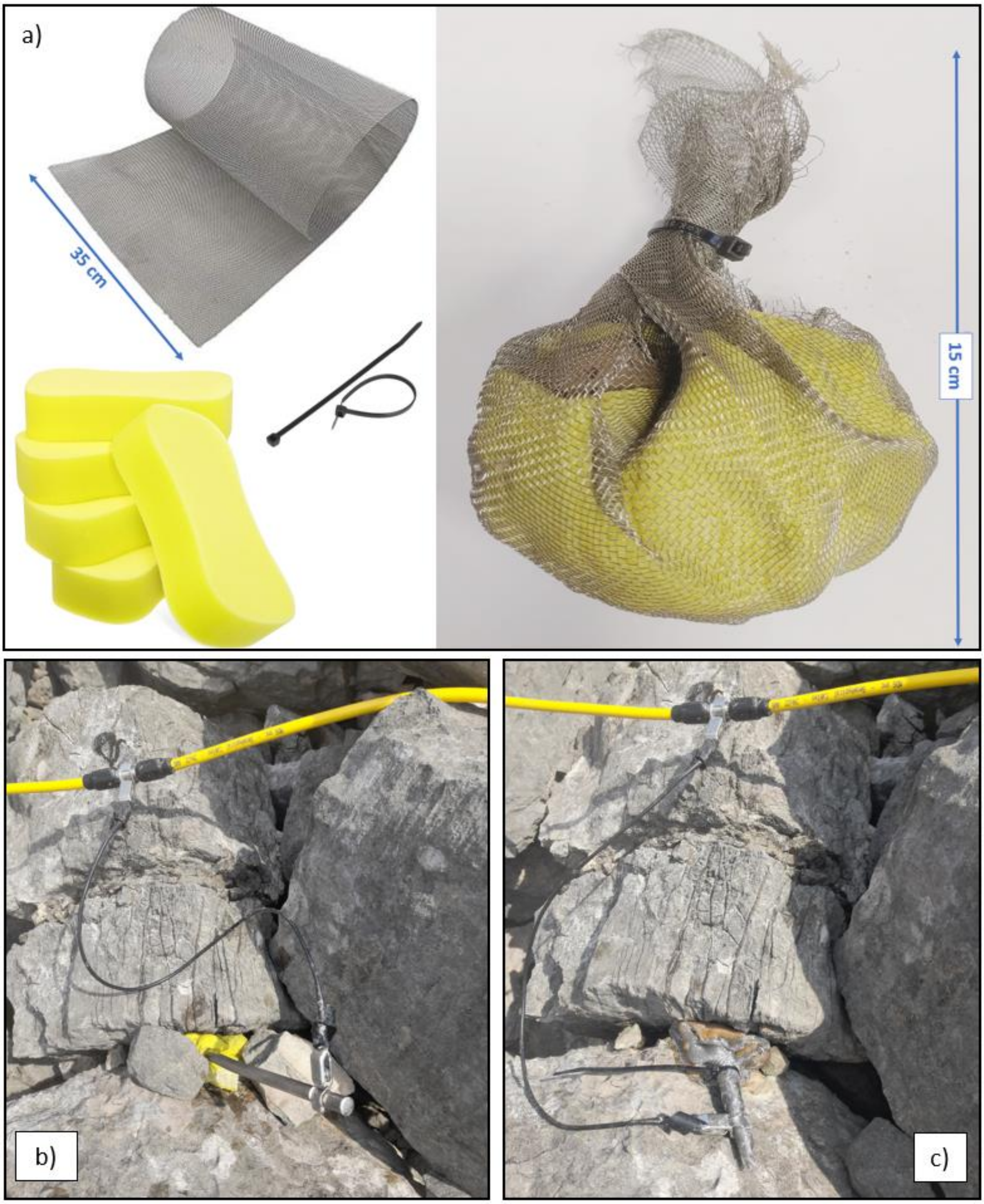

Figure 1: (a) Stainless steel net electrode assembled by cutting 35 × 35 cm squares from a thin commercial mesh, inserting a car-wash sponge, and securing the unit with a cable tie. (b) Traditional stainless steel spike electrode with a saltwater-soaked sponge, as used at the Marocche di Drò site. (c) Proposed stainless steel net electrode, also moistened with salt water, deployed at the same site.

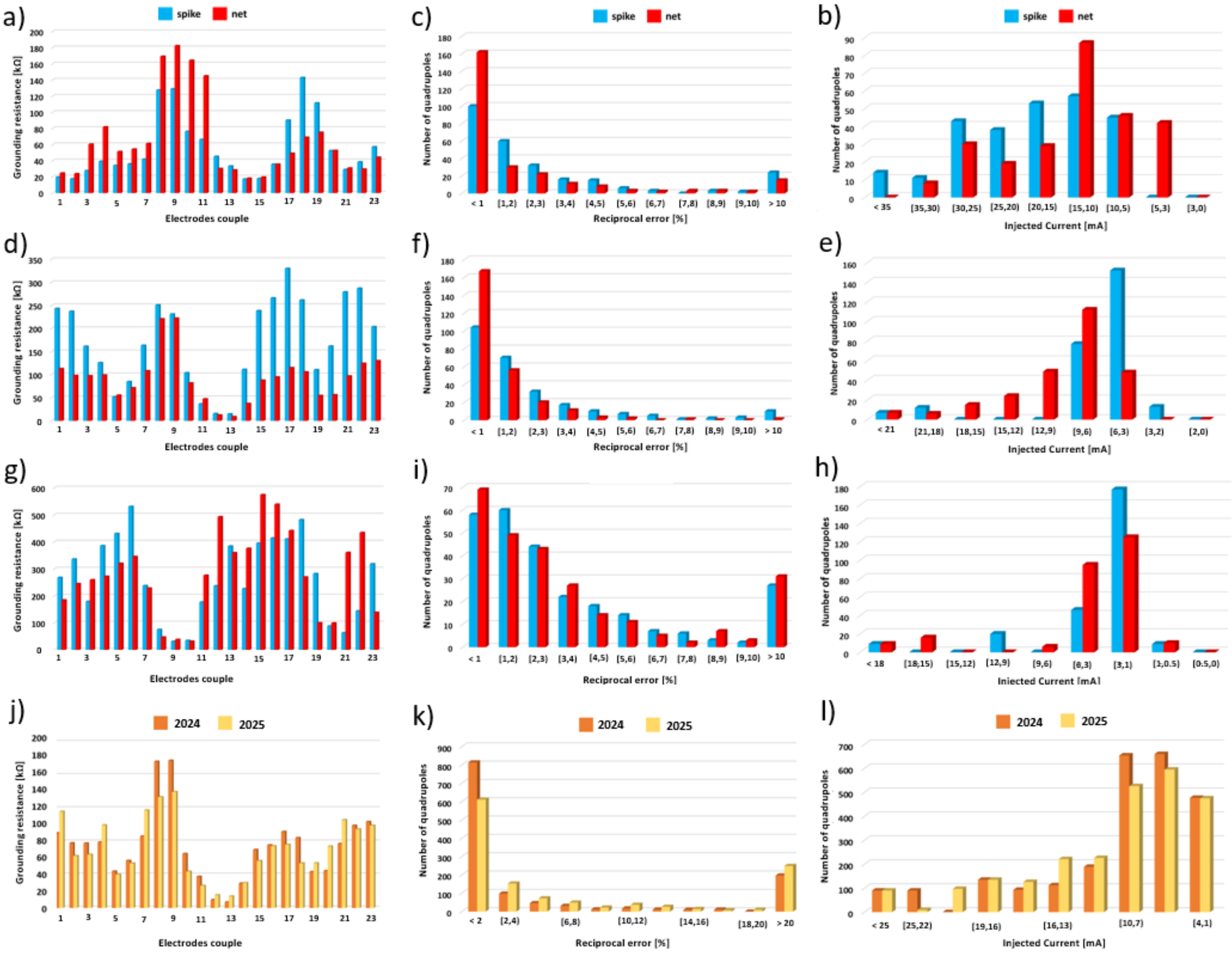

Figure 2. Histograms (a), (d), and (g) compare grounding resistances [kΩ] recorded at the Marocche di Drò, Sadole, and Flüela test sites, respectively, using traditional stainless-steel spike electrodes with sponges (blue) and the proposed stainless-steel net electrodes with sponge inserts (red). Panels (b), (e), and (h) show the corresponding injected electric currents [mA], while (c), (f), and (i) present the reciprocal error [%] of the quadrupoles for the same sites and electrode types. All electrodes were moistened with the same amount of saltwater and placed at comparable positions between surface boulders (see Fig. 1b–c). Panels (j), (k), and (l) illustrate the contact resistances (first 24 electrodes, as in panel a), injected currents, and reciprocal errors for datasets acquired at the Sadole site in June 2024 (orange) and June 2025 (yellow) along the permanent ERT monitoring line using the stainless-steel net electrodes.

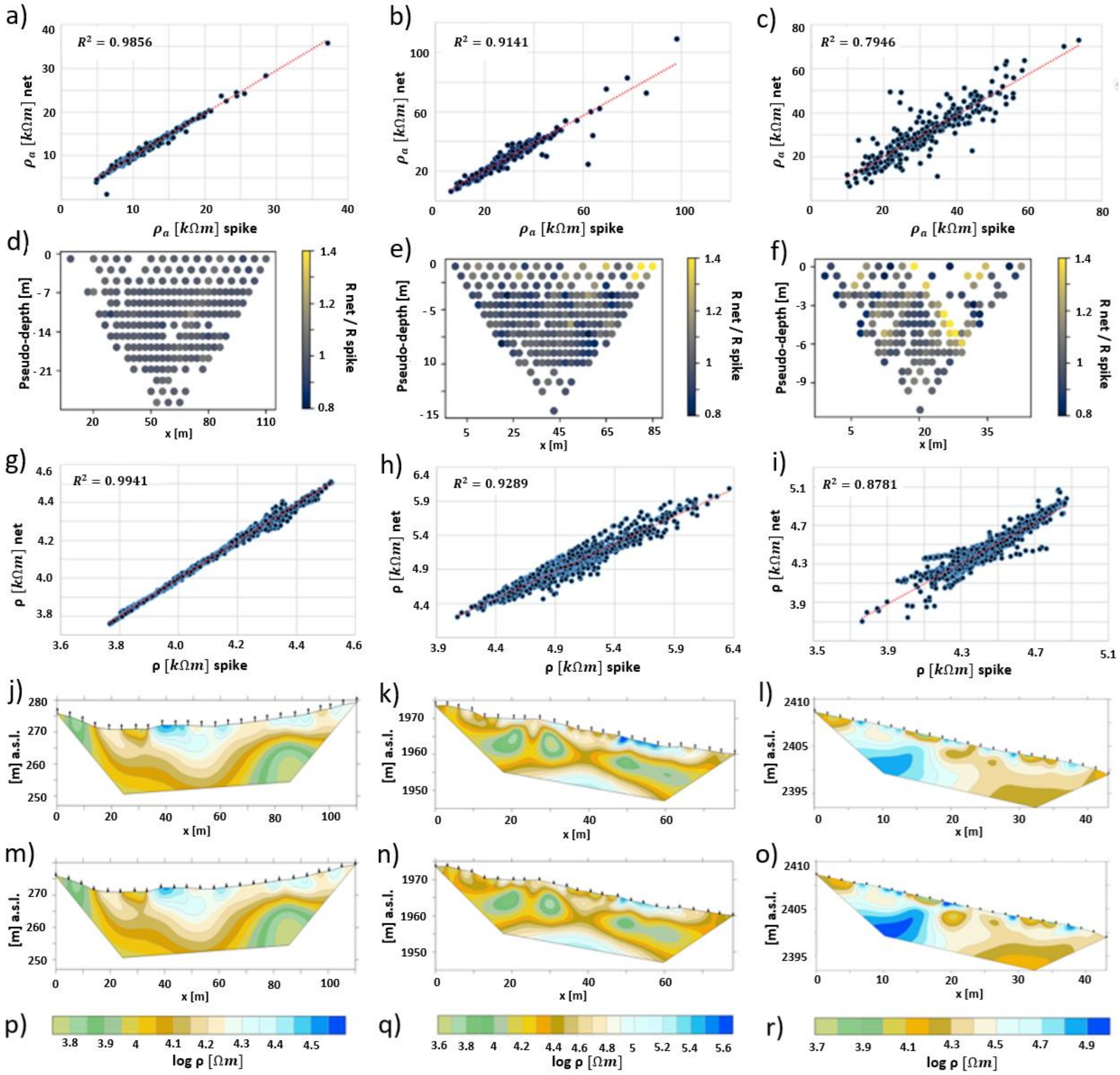

Figure 3. a) Scatterplot comparing apparent resistivity values (ρ_a) measured at the Marocche di Drò site using traditional stainless-steel spike electrodes (with sponges) and the proposed stainless-steel net electrodes. Red dashed lines indicate linear regressions, with corresponding R^2 values. d) Pseudosection showing the ratio of resistance values measured with spike electrodes to those measured with net electrodes, based on the common quadrupoles retained after data filtering for inversion. g) Scatterplot comparing inverted resistivity values (ρ) obtained from the two datasets at Marocche di Drò. Red dashed lines represent regression lines; R^2 values are shown. j) Inverted resistivity model derived from the spike-electrode dataset at Marocche di Drò. m) Inverted resistivity model derived from the net-electrode dataset at Marocche di Drò. p) Color scale used for the inverted resistivity models at the Marocche di Drò site. b), e), h), k), n), and q) correspond to a), d), g), j), m), and p), respectively, for the Sadole rock glacier test site. c), f), i), l), o), and r) correspond to a), d), g), j), m), and p), respectively, for the Flüela rock glacier test site.

Data Availability Statement. The datasets used to obtain the results presented in this work are available in the open-source repository https://zenodo.org/records/14651003. Furthermore, the ERT datasets will also be included in the International Database of Geoelectrical Surveys on Permafrost (IDGSP).

Author contributing. MP initiated and conceptualised the study concept and performed the data processing. All authors were involved in the data acquisition and contributed to the writing and editing of the manuscript.

Competing interests: The contact author has declared that none of the authors has any competing interests.

Financial support: This study was carried out within the project of the excellence program: “The Geosciences for Sustainable Development” project (Budget Ministero dell'Università e della Ricerca–Dipartimenti di Eccellenza 2023–2027 C93C23002690001), and within the project PRIN 2022 “SUBSURFACE – Ecohydrological and environmental significance of subsurface ice in alpine catchments” (code no. 2022AL7WKC, CUP: C53D23002020006), which received funding from the European Union NRRP (Mission 4, Component 2, Investment 1.1 – D. D. 104 2/2/2022).

Acknowledgements: We thank the editor, Professor Hördt, and two anonymous reviewers for their constructive comments and useful suggestions.

References

Bast, A., Pavoni, M., Lichtenegger, M., Buckel, J., and Boaga, J.: The Use of Textile Electrodes for Electrical Resistivity Tomography in Periglacial, Coarse Blocky Terrain: A Comparison With Conventional Steel Electrodes. Permafrost and Periglacial Processes, https://doi.org/10.1002/ppp.2257, 2024.

Binley, A.: Tools and Techniques: Electrical Methods, Treatise on Geophysics: Second Edition. Elsevier B.V. https://doi.org/10.1016/B978-0-444-53802-4.00192-5, 2015.

Binley, A., and Slater, L.: Resistivity and induced polarization: Theory and applications to the near-surface earth. Cambridge University Press, DOI: 10.1017/9781108685955, 2020.

Blanchy, G., Saneiyan, S., Boyd, J., McLachlan, P., and Binley, A.: ResIPy, an intuitive open source software for complex geoelectrical inversion/modeling. Computers & Geosciences, 137, 104423, https://doi.org/10.1016/j.cageo.2020.104423, 2020.

Boaga, J., Pavoni, M., Bast, A., and Weber, S.: Brief communication: On the potential of seismic polarity reversal to identify a thin low-velocity layer above a high-velocity layer in ice-rich rock glaciers. The Cryosphere, 18(7), 3231-3236, https://doi.org/10.5194/tc-18-3231-2024, 2024.

Boaga, J., Ghinassi, M., D’Alpaos, A., Deidda, G. P., Rodriguez, G., and Cassiani, G.: Geophysical investigations unravel the vestiges of ancient meandering channels and their dynamics in tidal landscapes. Scientific Reports, 8(1), 1708, DOI:10.1038/s41598-018-20061-5, 2018.

Buckel, J., Mudler, J., Gardeweg, R., Hauck, C., Hilbich, C., Frauenfelder, R., Kneisel, C., Buchelt, S., Blöthe, J. H., Hördt, A., and Bücker, M.: Identifying mountain permafrost degradation by repeating historical electrical resistivity tomography (ERT) measurements, The Cryosphere, 17, 2919–2940, https://doi.org/10.5194/tc-17-2919-2023, 2023.

Carrera, A., Peruzzo, L., Longo, M., Cassiani, G., and Morari, F.: Uncovering soil compaction: performance of electrical and electromagnetic geophysical methods. SOIL, 10(2), 843–857, https://doi.org/10.5194/soil-10-843-2024, 2024.

Deiana, R., Deidda, G. P., Cusí, E. D., van Dommelen, P., and Stiglitz, A.: FDEM and ERT measurements for archaeological prospections at Nuraghe S'Urachi (West-Central Sardinia). Archaeological Prospection, 29(1), 69-86. https://doi.org/10.1002/arp.1838, 2022.

Duba, A., Piwinskii, A. J., Santor, M., and Weed, H. C.: The electrical conductivity of sandstone, limestone and granite. Geophysical Journal International, 53(3), 583-597, https://doi.org/10.1111/j.1365-246X.1978.tb03761.x, 1978.

Pavoni, M., Carrera, A., and Boaga, J.: Improving the galvanic contact resistance for geoelectrical measurements in debris areas: A case study. Near Surface Geophysics, 20(2), 178-191, https://doi.org/10.1002/nsg.12192, 2022.

Pavoni, M., Boaga, J., Carrera, A., Zuecco, G., Carturan, L., and Zumiani, M.: Brief communication: Mountain permafrost acts as an aquitard during an infiltration experiment monitored with electrical resistivity tomography time-lapse measurements. The Cryosphere, 17(4), 1601-1607, https://doi.org/10.5194/tc-17-1601-2023, 2023.

Pavoni, M., Boaga, J., Peruzzo, L., Barone, I., Mary, B., & Cassiani, G.: Characterization of a Contaminated Site Using Hydro-Geophysical Methods: From Large-Scale ERT Surface Investigations to Detailed ERT and GPR Cross-Hole Monitoring. Water, 16(9), 1280, https://doi.org/10.3390/w16091280, 2024.

Peruzzo, L., Chou, C., Hubbard, S., Brodie, E. L., Uhlemann, S., Dafflon, B., and Wu, Y.: Outdoor Mesoscale Fabricated Ecosystems: Rationale, Design, and Application to Evapotranspiration. Design, and Application to Evapotranspiration, https://doi.org/10.1016/j.scitotenv.2024.177565, 2024.

Reynolds, J. M.: An introduction to applied and environmental geophysics. John Wiley & Sons, ISBN 9778-0-471-48535-3, 2011.

Rücker, C., and Günther, T.: The simulation of finite ERT electrodes using the complete electrode model. Geophysics, 76(4), F227-F238. https://doi.org/10.1190/1.3581356, 2011.

Rücker, C., Günther, T., and Wagner, F. M.: pyGIMLi: An open-source library for modelling and inversion in geophysics. Computers & Geosciences, 109, 106-123, https://doi.org/10.1016/j.cageo.2017.07.011, 2017.

Tso, C. H. M., Kuras, O., Wilkinson, P. B., Uhlemann, S., Chambers, J. E., Meldrum, P. I., ... and Binley, A..: Improved characterisation and modelling of measurement errors in electrical resistivity tomography (ERT) surveys. Journal of Applied Geophysics, 146, 103-119, https://doi.org/10.1016/j.jappgeo.2017.09.009, 2017.

Uhlemann, S., Peruzzo, L., Chou, C., Williams, K. H., Wielandt, S., Wang, C., ... and Dafflon, B.: Variations in bedrock and vegetation cover modulate subsurface water flow dynamics of a mountainous hillslope. Water Resources Research, 60(2), e2023WR036137, https://doi.org/10.1029/2023WR036137, 2024.

Weidinger, J.T., Korup, O., Munack, H., Altenberger, U., Dunning, S.A., Tippelt, G., and Lottermoser, W.: Giant rock slides from the inside. Earth and Planetary Science Letters 389, 62–73, https://doi.org/10.1016/j.epsl.2013.12.017, 2014.